

Multidimensional Modelling of Cross-Beam Energy Transfer for Direct-Drive Inertial Confinement Fusion

(Hopefully soon to be Dr.) Philip W. X. Moloney

IMPERIAL

June 2024

Submitted in partial fulfilment of the requirements for the degree of
Doctor of Philosophy of Imperial College London

Department of Physics
Imperial College London
Prince Consort Road
London SW7 2AZ

List of Acronyms

Rad-MHD Radiative-Magnetohydrodynamics

MHD Magnetohydrodynamics

LPIs Laser-Plasma Instabilities

CBET Cross-Beam Energy Transfer

ICF Inertial Confinement Fusion

IAW Ion Acoustic Wave

1 Simulations of Cross-Beam Energy Transfer for Magnetised Direct-Drive

This chapter describes a set of simulations which were conducted to understand the role of Cross-Beam Energy Transfer (CBET) in magnetised, direct-drive implosions. Magnetised Inertial Confinement Fusion (ICF) is a promising route to achieving higher target gains, due to the reduction of thermal energy loss at stagnation and additional confinement of the alpha particles responsible for burn propagation. For direct-drive implosions, magnetisation can significantly alter the coronal plasma profiles, due to the introduced anisotropy of thermal transport. The Ion Acoustic Wave (IAW) dispersion relation, which mediates CBET interactions, depends upon the background plasma and therefore significantly altered temperature and density profiles could alter the action of CBET. Before the development of SOLAS, no direct-drive suitable CBET model existed, which was integrated into a Radiative-Magnetohydrodynamics (Rad-MHD) code. Therefore, the CHIMERA-SOLAS computational model has allowed the effect of magnetisation on CBET to be studied for a direct-drive implosion.

The chapter begins with a review of experimental and computational work on magnetised ICF, with a particular focus on magnetised direct-drive. Work presented in this chapter focuses on the study of *exploding-pusher* experiments. These are very different implosions to the typical *central hot-spot* ignition designs, presented in previous chapters, so a short summary of exploding pushers is also provided. Simulation results are presented of 1-D and 2-D, unmagnetised exploding pushers, both with and without the effect of CBET, which demonstrate that CBET does significantly alter the implosion. This is followed by an investigation of how various extended-Magnetohydrodynamics (MHD) terms affect the implosion, including the Nernst effect, the Lorentz force and resistive diffusion of the magnetic field. Results are given of how magnetisation affects the CBET interaction and ultimately how it changes the stagnation shape of the target. The results presented, demonstrate that redistribution of deposited power due to CBET, reduced the amplitude of the stagnation asymmetry, which originated from the polar beam configuration used, due to the presence of a field coil at the equator. However, the reduction of asymmetry was consistent for different initial seed magnetic field values, and therefore CBET was not observed to be sufficiently strongly affected by magnetisation, to lead to observable signatures in experimental measurements. The chapter concludes with a summary of the work and suggestions of additional experimental configurations, which may leave a more significant signature of magnetisation altering CBET.

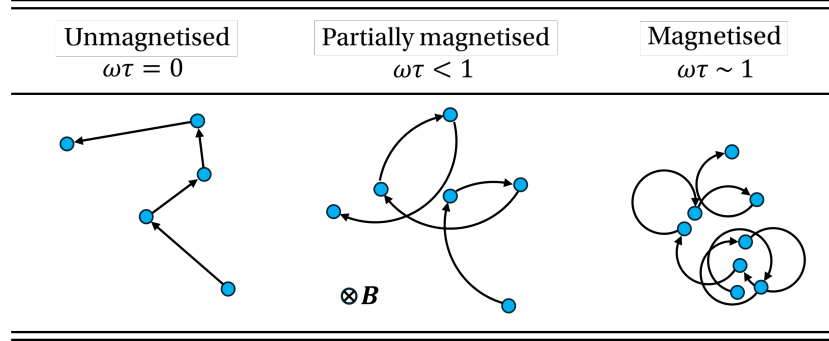


Figure 1.1: lol.

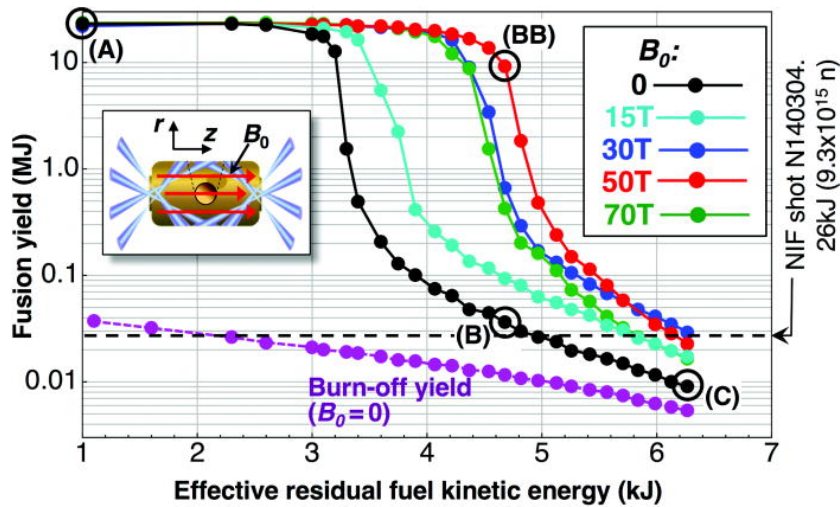


Figure 1.2: lol. Reused with permission from Ref. [1].

1.1 Magnetised Inertial Confinement Fusion and Exploding Pushers

This chapter begins with a review of published work that is relevant to the simulations which are presented. Firstly, a short review of magnetised-ICF is presented which reviews both the key concepts, existing studies and potential challenges of the design. Both work on direct- and indirect drive is summarised, alongside recent theoretical progress on understanding how magnetisation can effect Laser-Plasma Instabilities (LPIs). The exploding pusher concept is then briefly explored to aid understanding of the implosion physics, which is markedly different to conventional hot-spot ICF.

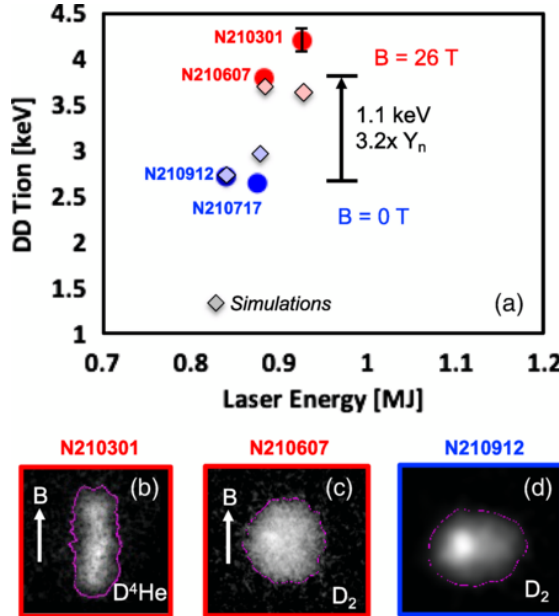


Figure 1.3: lol. Reused with permission from Ref. [2].

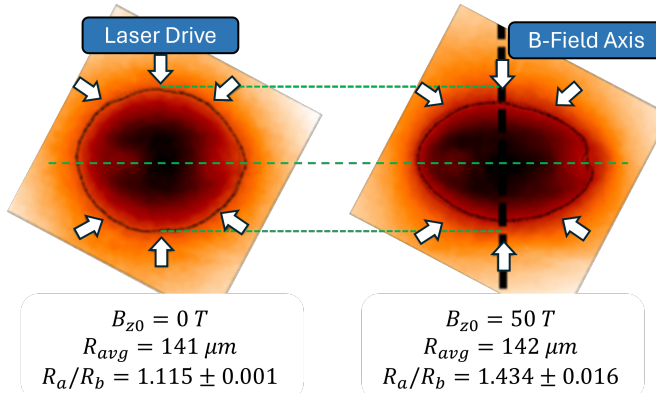


Figure 1.4: lol. Adapted with permission from Ref. [3].

1.1.1 Potential Benefits of Magnetisation

1.1.2 Existing Studies of Magnetised-ICF

1.1.3 Magnetised Laser-Plasma Instabilities

1.1.4 The Exploding-Pusher Configuration

1.1.5 Simulation Configuration

1.2 Effect of Cross-Beam Energy Transfer in Unmagnetised Exploding Pushers

This section presents simulation results of the effect of CBET in exploding pushers on OMEGA. Both 1-D and 2-D CHIMERA-SOLAS simulations of 40-beam, polar driven exploding pusher experiments are presented, with a focus on how CBET acts to change the implosion. The 1-D

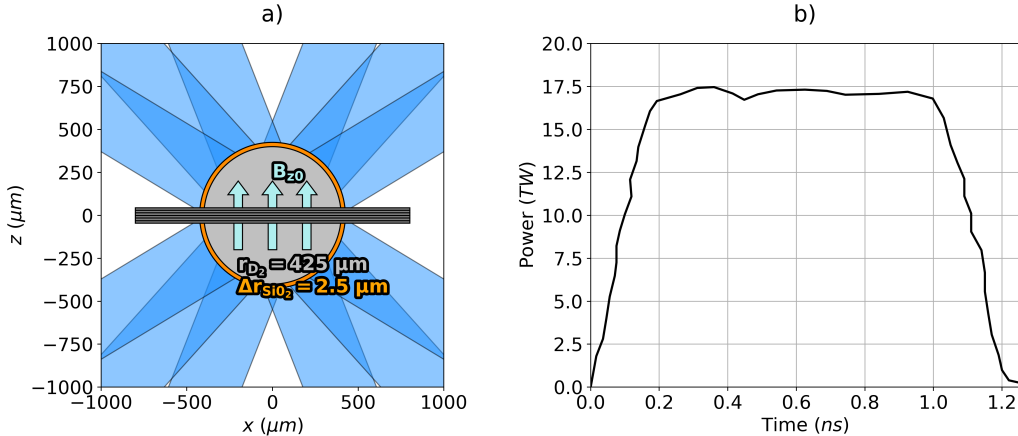


Figure 1.5: lol.

results demonstrate that CBET significantly reduces the coupled laser energy to the implosion from ... to Simulations conducted in 2-D, with a full 3-D raytrace and CBET model, show that CBET alters spatial profile of the laser deposition, reducing asymmetry in the drive.

1.2.1 1-D Simulations

1.2.2 2-D Simulations

1.3 The Effect of Magnetisation on Exploding-Pusher Implosions

This section presents results of a study of the effect that extended-MHD has on the 2-D exploding pusher simulations. Simulations were conducted with varying initial magnetic field strengths and particular terms turned off and on to deduce what the important physical processes are. Magnetised transport is important for both initial seed magnetic field implosions, resulting in large coronal Hall parameters and therefore significant anisotropy of the implosions. The results demonstrate that (resistive diffusion and the Lorentz force have very little impact on the implosion physics, due to the bulk of the plasma being highly resistive and high-\$\beta\$ respectively)?????????????????????. The Nernst advection of magnetic field ??????????????????????

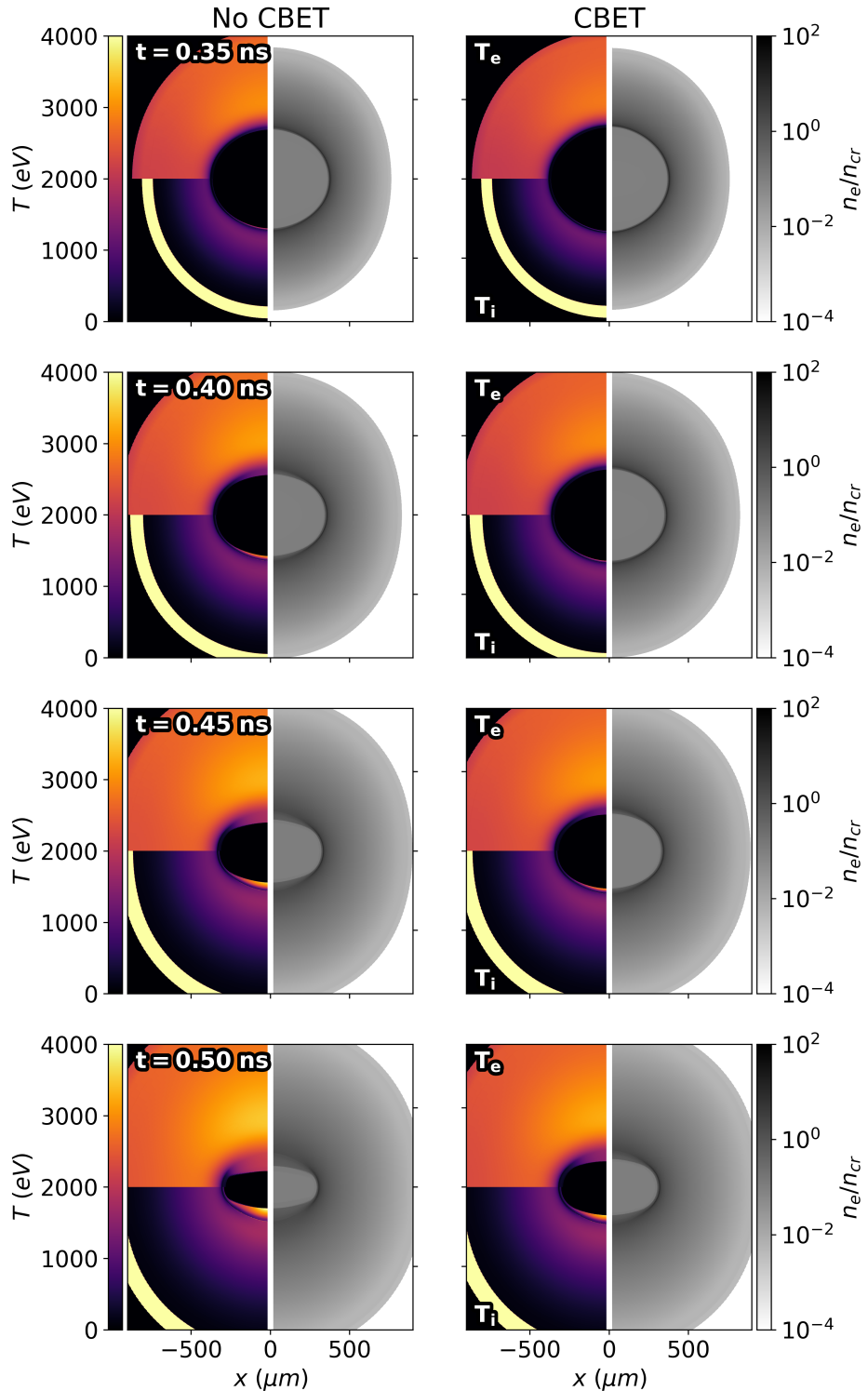


Figure 1.6: lol.

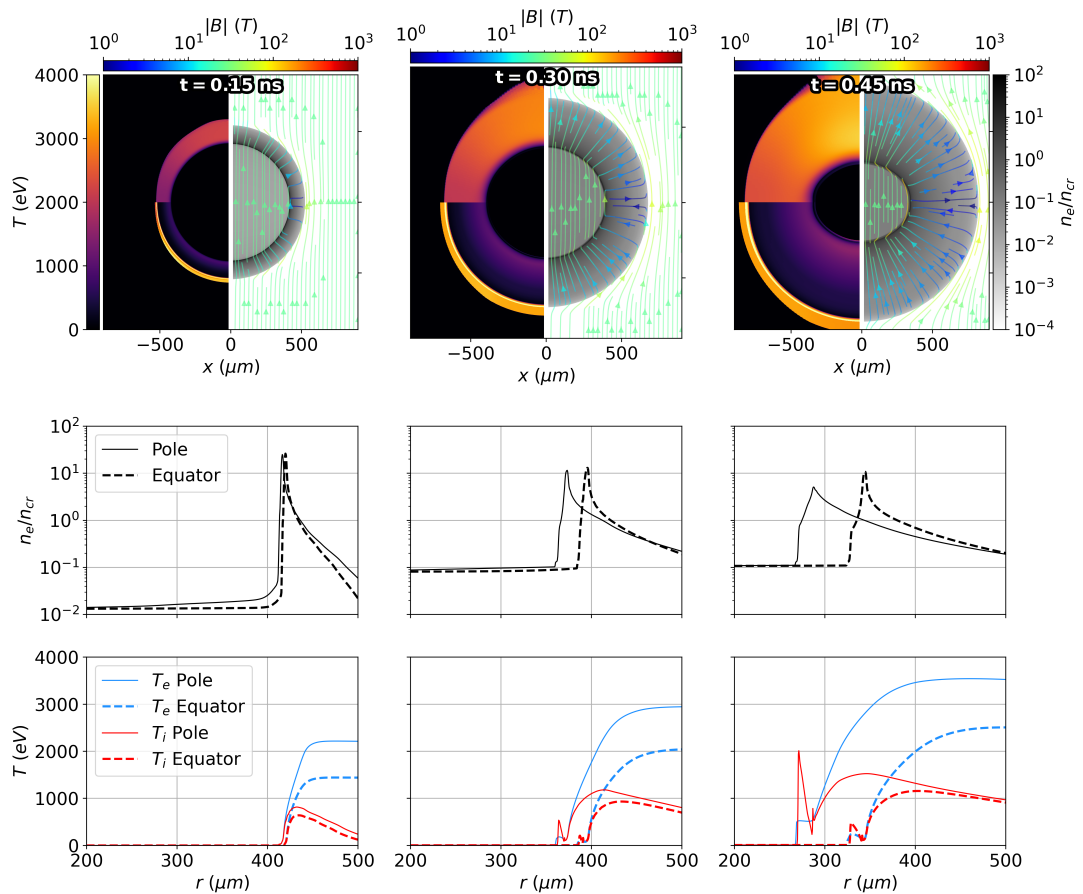


Figure 1.7: lol.

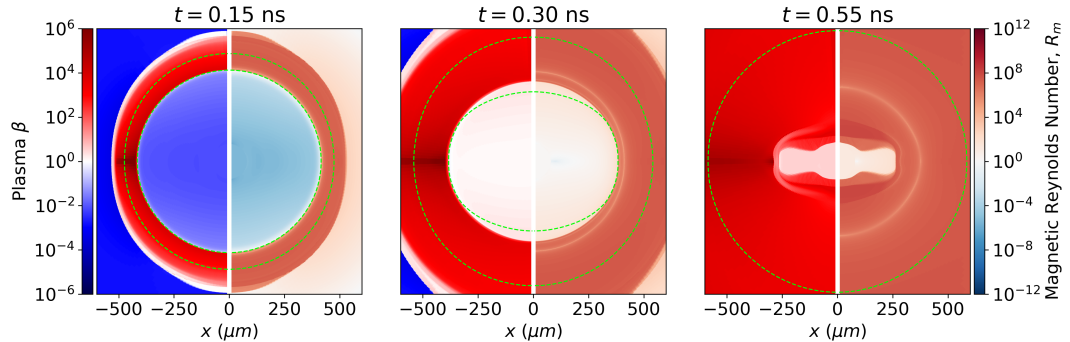


Figure 1.8: lol.

1.3.1 In-Flight Field Structure

1.3.2 Anisotropic Thermal Conduction

1.3.3 The Nernst Effect

1.3.4 Resistive Diffusion and the Lorentz Force

1.4 The Effect of Magnetisation on Cross-Beam Energy Transfer and Stagnation

This section presents results on how the magnetisation of the corona affects both CBET scattering and the stagnation shape of the implosion. As was shown in the previous sec-

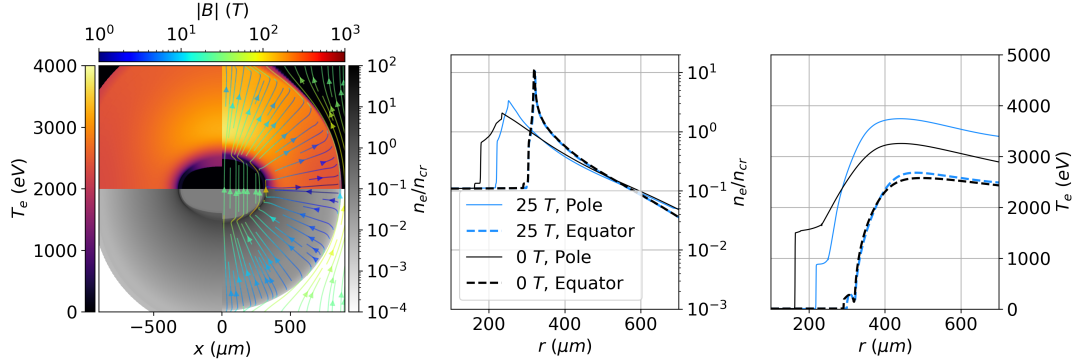


Figure 1.9: lol.

tions, the laser geometry leads to a significant mode $\ell = 2$ in the coronal plasma conditions, which is significantly amplified by anisotropic thermal conduction when magnetised. This long-wavelength perturbation is slightly reduced by CBET, consistent with existing literature on how CBET mitigates $\ell = 1$ asymmetries [4]. ‘No-CBET’ simulations were conducted, for which the coupled energy was kept the same as the equivalent CBET simulation, *i.e.* so CBET only acted to redistribute the deposited power, rather than reduce its magnitude. These results showed that the increasingly anisotropic coronal plasma profiles for increasing seed magnetic field strengths did lead to changes in the CBET scattering, this was too small an effect to lead to experimentally observable changes in behaviour.

1.4.1 Analysis and Key Definitions

1.4.2 Spatial Change of CBET and Deposition from Magnetisation

1.4.3 Stagnation Profiles

1.5 Conclusions

1.5.1 Summary of Work

1.5.2 Future Work

Table 1.1: Results of all Simulations. In the CBET column, ‘~’ indicates CBET affecting the magnitude, but *not* spatial location, of deposition.

Run	Dim.	CBET	Note	B_{z0} (T)	t_b (ns)	$\langle T_i \rangle$ (keV)	Y_n ($\times 10^{10}$)	Δ_b (ps)	R_2/R_1
1	1-D	Off	-	0	0.69	14.66	11.62	87	$1.00^{+0.00}_{-0.00}$
2	1-D	On	-	0					$1.00^{+0.00}_{-0.00}$
3	2-D	Off	-	0	0.71	8.44	6.20	148	$2.96^{+0.20}_{-0.19}$
4	2-D	~	-	0	0.75	7.61	5.23	153	$3.26^{+0.25}_{-0.23}$
5	2-D	On	-	0	0.75	7.77	5.46	148	$3.23^{+0.25}_{-0.23}$
6	2-D	Off	-	25	0.74	7.26	4.73	130	$3.80^{+0.41}_{-0.33}$
7	2-D	~	-	25	0.78	6.58	4.14	125	$4.55^{+0.50}_{-0.43}$
8	2-D	On	-	25	0.78	6.72	4.44	123	$4.32^{+0.47}_{-0.41}$
9	2-D	Off	-	50	0.73	6.82	3.73	134	$4.40^{+0.43}_{-0.38}$
10	2-D	~	-	50	0.78	6.30	3.30	130	$4.92^{+0.56}_{-0.48}$
11	2-D	On	-	50	0.78	6.37	3.52	129	$4.79^{+0.55}_{-0.47}$
12	2-D	Off	No Aniso.	25	0.81	6.40	5.02	118	$3.14^{+0.68}_{-0.50}$
13	2-D	Off	No Lor.	25	0.74	7.29	4.77	131	$3.80^{+0.41}_{-0.33}$
14	2-D	Off	No Nern.	25	0.73	7.41	4.85	130	$3.74^{+0.38}_{-0.32}$
15	2-D	Off	No Resis.	25	0.73	7.07	4.59	132	$3.84^{+0.42}_{-0.33}$

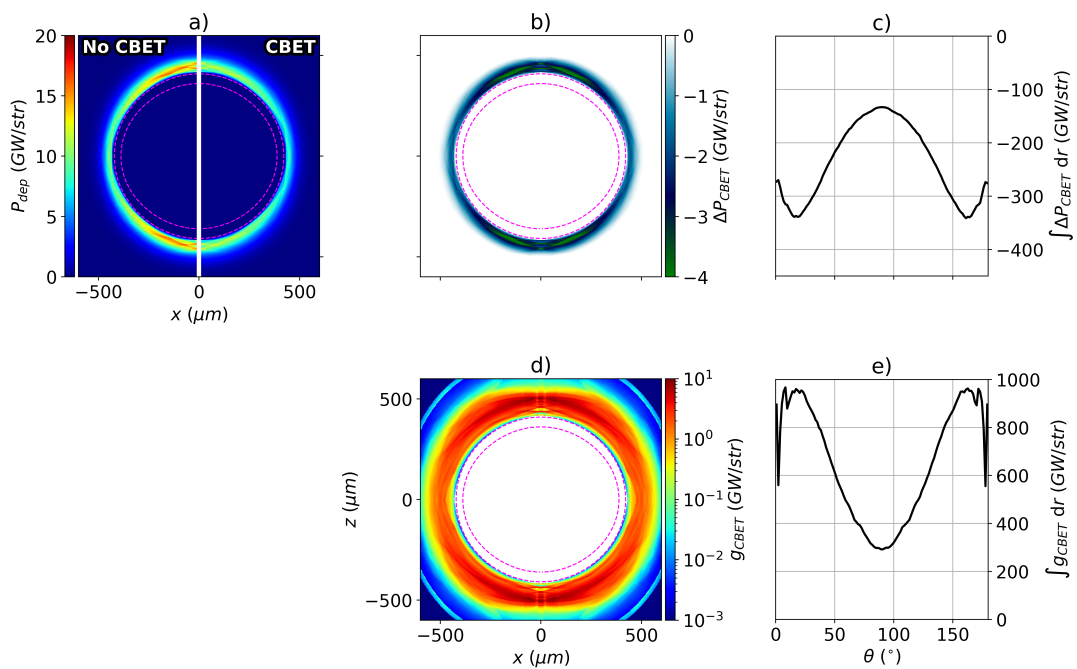


Figure 1.10: lol.

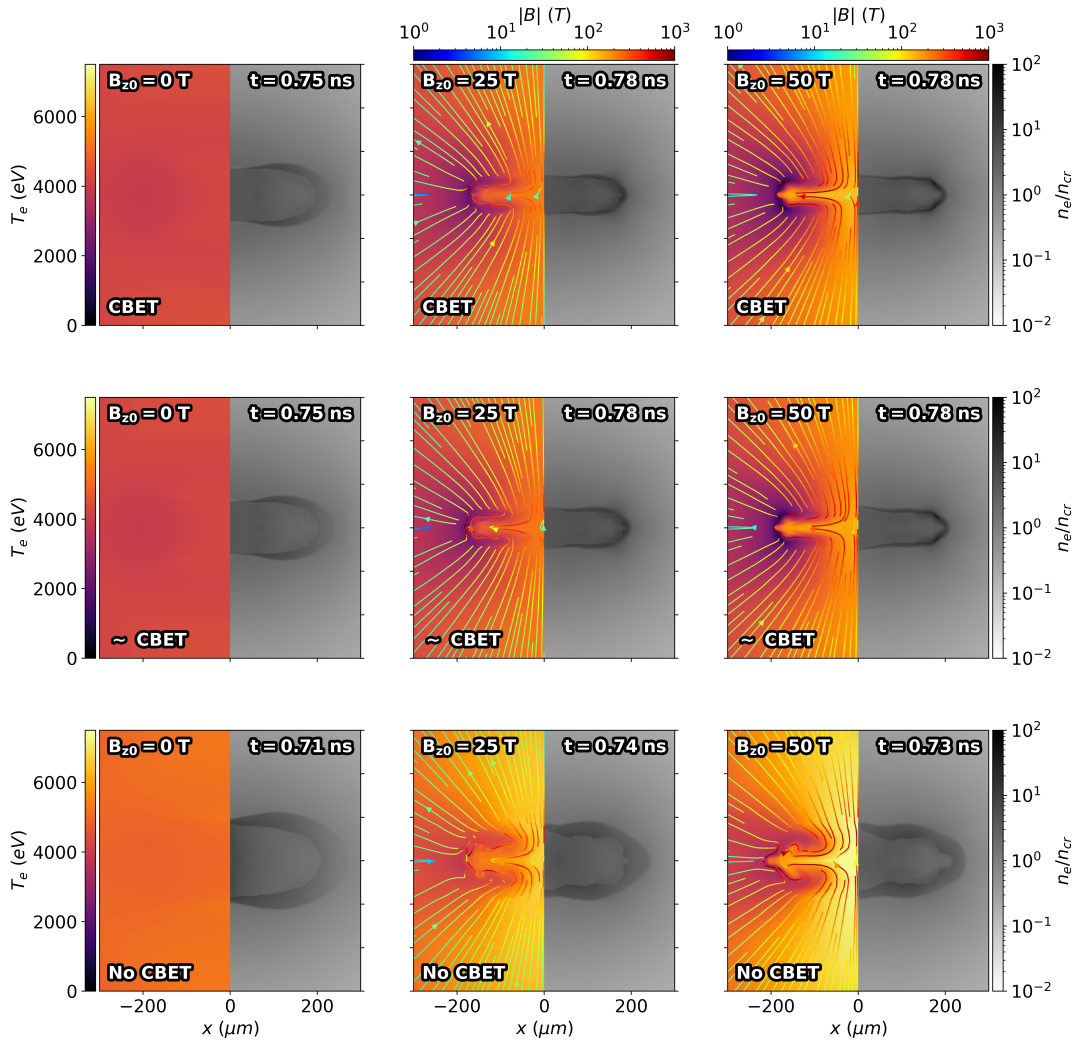


Figure 1.11: lol.

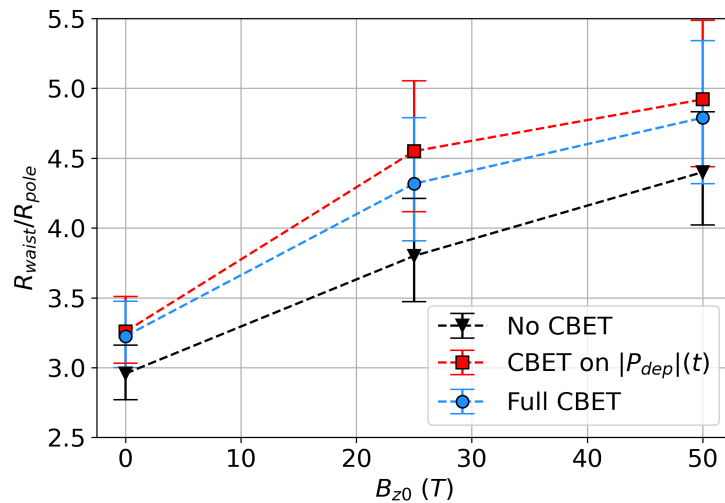


Figure 1.12: lol.

Appendices

Bibliography

- [1] L. J. Perkins, D. D.-M Ho, B. G. Logan, G. B. Zimmerman, M. A. Rhodes, D. J. Strozzi, D. T. Blackfield, and S. A. Hawkins. The potential of imposed magnetic fields for enhancing ignition probability and fusion energy yield in indirect-drive inertial confinement fusion. *Physics of Plasmas*, 24(6):062708, June 2017. ISSN 1070-664X, 1089-7674. doi: 10.1063/1.4985150. URL <https://pubs.aip.org/pop/article/24/6/062708/108192/The-potential-of-imposed-magnetic-fields-for>. 6
- [2] J. D. Moody, B. B. Pollock, H. Sio, D. J. Strozzi, D. D.-M. Ho, C. A. Walsh, G. E. Kemp, B. Lahmann, S. O. Kucheyev, B. Kozioziemski, E. G. Carroll, J. Kroll, D. K. Yanagisawa, J. Angus, B. Bachmann, S. D. Bhandarkar, J. D. Bude, L. Divol, B. Ferguson, J. Fry, L. Hagler, E. Hartouni, M. C. Herrmann, W. Hsing, D. M. Holunga, N. Izumi, J. Javedani, A. Johnson, S. Khan, D. Kalantar, T. Kohut, B. G. Logan, N. Masters, A. Nikroo, N. Orsi, K. Piston, C. Provencher, A. Rowe, J. Sater, K. Skulina, W. A. Stygar, V. Tang, S. E. Winters, G. Zimmerman, P. Adrian, J. P. Chittenden, B. Appelbe, A. Boxall, A. Crilly, S. O'Neill, J. Davies, J. Peebles, and S. Fujioka. Increased Ion Temperature and Neutron Yield Observed in Magnetized Indirectly Driven D 2 -Filled Capsule Implosions on the National Ignition Facility. *Physical Review Letters*, 129(19):195002, November 2022. ISSN 0031-9007, 1079-7114. doi: 10.1103/PhysRevLett.129.195002. URL <https://link.aps.org/doi/10.1103/PhysRevLett.129.195002>. 7
- [3] A. Bose, J. Peebles, C. A. Walsh, J. A. Frenje, N. V. Kabadi, P. J. Adrian, G. D. Sutcliffe, M. Gatu Johnson, C. A. Frank, J. R. Davies, R. Betti, V. Yu. Glebov, F. J. Marshall, S. P. Regan, C. Stoeckl, E. M. Campbell, H. Sio, J. Moody, A. Crilly, B. D. Appelbe, J. P. Chittenden, S. Atzeni, F. Barbato, A. Forte, C. K. Li, F. H. Seguin, and R. D. Petrasso. Effect of Strongly Magnetized Electrons and Ions on Heat Flow and Symmetry of Inertial Fusion Implosions. *Physical Review Letters*, 128(19):195002, May 2022. ISSN 0031-9007, 1079-7114. doi: 10.1103/PhysRevLett.128.195002. URL <https://link.aps.org/doi/10.1103/PhysRevLett.128.195002>. 7
- [4] A. Colaïtis, I. Igumenshchev, J. Mathiaud, and V. Goncharov. Inverse ray tracing on icosahedral tetrahedron grids for non-linear laser plasma interaction coupled to 3D radiation hydrodynamics. *Journal of Computational Physics*, 443:110537, October 2021. ISSN 0021-9991. doi: 10.1016/j.jcp.2021.110537. URL <https://www.sciencedirect.com/science/article/pii/S0021999121004320>. 11

Permissions